Clay Concentration Dependence of Microstructure in Deformed Poly(*N*-isopropylacrylamide)−Clay Nanocomposite Gels

Sho Miyazaki,[†] Takeshi Karino,[†,‡] Hitoshi Endo,[†] Kazutoshi Haraguchi,[§] and Mitsuhiro Shibayama*[,†,‡]

Neutron Science Laboratory, Institute for Solid State Physics, University of Tokyo, Tokai, Ibaraki 319-1106, Japan, CREST, Japan Science and Technology Agency, 4-1-8 Honcho Kawaguchi, Saitama 332-0012, Japan, and Kawamura Institute of Chemical Research, 631 Sakada, Sakura-shi, Chiba 285-0078, Japan

Received July 25, 2006; Revised Manuscript Received September 13, 2006

ABSTRACT: The microscopic structure of poly(*N*-isopropylacrylamide)−clay nanocomposite gels (NC gels) having various clay concentrations (C_{clay}) was investigated by mechanical measurement and small-angle neutron scattering (SANS) as a function of stretching ratio λ. The mechanical measurements indicated that the number of poly(*N*-isopropylacrylamide) (PNIPA) chains bridging clay platelets, N_{chain}, per unit volume increased with $C_{clay}^{4/3}$. Two-dimensional SANS intensity patterns exhibited the so-called "abnormal-butterfly" pattern. However, both sector-averaged scattering intensities parallel and perpendicular to the stretching direction were well represented by Ornstein−Zernike (OZ) scattering functions, suggesting that the NC gels have very little cross-linking inhomogeneities regardless of C_{clay} and of λ ($\lambda \leq 2.0$). The correlation length, ξ, obtained by the OZ functions was a decreasing function of C_{clay}, i.e., $\xi \sim C_{clay}^{-1/3}$, and was in proportion to the inter-platelet distance ($\sim C_{clay}^{-1/3}$). This suggests that the concentration fluctuations are effectively screened by clay platelets. The additional C_{clay} dependence in N_{chain}, i.e., $N_{chain}/C_{clay} \sim C_{clay}^{1/3}$, is due to localization of cross-links to the two-dimensional space on clay platelets. This is one of the direct evidence of "plane" cross-linking, which contributes to the advanced mechanical properties of NC gels.

Introduction

Polymer−clay nanocomposite materials have lately attracted considerable attention because of their high mechanical properties, heat resistance, and so on.[1,2] Here, clay is not only a reinforcement but also an important constituent in improving the physical properties of the nanocomposites. Recently, Haraguchi et al. developed novel polymer−clay nanocomposite gels (hereafter we call NC gel).[3−7] The NC gels are made by free-radical polymerization of *N*-isopropylacrylamide (NIPA) in the presence of synthetic clay, Laponite. Transmission electron micrographs of dried NC gels clearly showed fine dispersion of exfoliated clay platelets.[4] X-ray diffraction patterns of NC gels having low polymer content showed a distinct Bragg peak originating from a stacking of clay, and the peak shifted to lower angles by increasing polymer content, indicating a random orientation of clay platelets.[6] These results clearly indicate fine dispersion of clay platelets in the polymer matrix. As a result, NC gels have high extensibility and strong toughness owing to a cross-linked polymer network structure via clay platelets as reported elsewere.[3,8] Such advanced properties cannot be obtained in conventional chemical gels or physical gels. NC gels, on the other hand, have various useful physical properties, such as high deformability, incredibly high toughness, high transparency even at high clay content, a high degree of swelling capability, etc. In our previous papers, we investigated the structure and dynamics of NC gels in order to clarify the origins of the advanced mechanical properties.[9,10] Nie et al. also discussed the relationship between mechanical/swelling properties and structures by focusing on spatial inhomogeneities and dynamic fluctuations.[11,12]

In general, gels are made of a small fraction of polymer component and a large portion of solvent. Hence, gels are very eco-friendly material and are served in various applications. Though high toughness and mechanical strength in gels have been anticipated, conventional gels are very brittle and fragile. Hence, the advanced mechanical properties of NC gels are expected to expand the applicability of conventional gel. The most interesting fact is that the improved properties are obtained by simply replacing *N,N′*-methylenebis(acrylamide) (BIS) (cross-linker of usual chemical gels) with clay in a pregel solution. Note that a simple mixture of PNIPA and clay in water does not behave like NC gels.

In the previous paper,[10] we reported the microscopic structure of stretched NC4 (here the number 4 indicating the clay concentration C_{clay} of 0.04 M) investigated with small-angle neutron scattering (SANS). The NC gels were found to have (1) a lower level of cross-link inhomogeneities and (2) "plane cross-linker" compared with BIS as "point cross-linker". The latter statement agrees well with the concept of "multifunctional cross-linking" reported by Oppermann and coworkes.[12] These two characteristic features were confirmed to be the most important factors to generate the amazing mechanical properties of NC gels. It is of importance to examine how these properties vary with C_{clay}. Hence, it is the objective of this paper to investigate C_{clay} dependence on the microscopic structure and to relate it to the mechanical properties.

Experimental Section

Samples. Three types of NC gels were prepared by free-radical polymerization of *N*-isopropylacrylamide (NIPA) monomer in the presence of synthetic clay, Laponite XLG ($[Mg_{5.34}Li_{0.66}Si_8O_{20}(OH)_4]$-$Na_{0.66}$). We used potassium peroxodisulfate (KPS) and *N,N,N′,N′*-

* To whom corresponding should be addressed. E-mail: shibayama@issp.u-tokyo.ac.jp.
† Neutron Science Laboratory, Institute for Solid State Physics, University of Tokyo.
‡ CREST, Japan Science and Technology Agency.
§ Kawamura Institute of Chemical Research.

10.1021/ma061688o CCC: $33.50 © 2006 American Chemical Society
Published on Web 10/21/2006

tetramethylethylenediamine (TEMED) as an initiator and catalyst, respectively. The NIPA monomer concentration was 690 mM (7.8 wt %). The details of the preparation procedure are given elsewhere.[10] NC gels for SANS experiments were polymerized in a sealed Teflon mold of 2 cm wide, 4 cm long, and 4 mm thick at 20 °C for 20 h. Thus, prepared slab gels were set to a custom-made stretching device. The sample codes were defined by the ratio of the clay and water, i.e., NC2, NC4, and NC6. This indicates 0.02, 0.04, and 0.06 mol of clay (=15.24, 30.48, and 45.72 g) in 1 L of D_2O or mixed water whose scattering length density was adjusted to the same as that of clay (the volume fraction was H_2O:D_2O = 0.34:0.66). We confirmed that the scattering length density of the H_2O/D_2O mixed water as mentioned above was close enough to that of the clay.[10] In addition, samples (NC2, NC4, and NC6) for dynamic light scattering (DLS) experiments were prepared in a test tube under nitrogen gas purge. For comparison, a conventional PNIPA gel cross-linked with *N*,*N*′-methylenebis(acrylamide) (BIS) was also prepared. The BIS concentration was 3.00 mol % with respect to NIPA monomer and the NIPA concentration was 1 M. Hence, we call this gel an organic gel (OR3). The mass densities of the clay and dry PNIPA were evaluated to be 2.65 and 1.26 g/cm^3.[3]

Mechanical Measurements. Tensile mechanical measurements were performed on NC and OR gels of the same size (5.5 mm, 70 mm length) and the same water/polymer ratio (10/1 (w/w)) using a Shimadzu Autograph AGS-H. Tensile properties of NC gels were obtained under the following conditions; sample length between jaws 35 mm; crosshead speed 100 mm min^{-1}; test temperature 25 °C. The initial cross section (23.75 mm^2) was used to calculate the tensile strengths and the tensile moduli.[4]

Small-Angle Neutron Scattering (SANS). SANS experiments were performed at the SANS instrument (SANS-U), Institute for Solid State Physics, the University of Tokyo.[13] The neutron wavelength was 7.0 Å and its distribution was ca. 10%. The sample-to-detector distance (SDD) was 2.00 and 8.00 m to cover a wide range of the scattering vector, q. The scattered neutrons were collected with a two-dimensional detector (model 2660N, Ordela) and then necessary corrections were made, such as air scattering, cell scattering, and incoherent background subtraction. After these corrections, the scattered intensity was normalized to the absolute intensity in terms of the scattering intensity from a standard sample. Data reduction was carried out by circular-averaging or by sector-averaging of the two-dimensional intensity data, followed by incoherent scattering subtraction.[14] The temperature of the samples was regulated to be 20 °C with a water-circulating bath controlled with a Neslab RTE−111 thermocontroller with the precision of ±0.1 °C. The stretching experiment was conducted with the same manner as was employed in the previous paper.[10] The sample was stretched stepwise with the step of $\Delta\lambda = 0.2$ (up to $\lambda = 2.0$), and then $\Delta\lambda = 1.0$ (from $\lambda = 2.0$ up to $\lambda = 6.0$). Here, λ ($\equiv l/l_0$) is the stretching ratio, and l_0 and l are the sample lengths before and after stretching, respectively. The humidity of the sample environment was kept constant by placing a bottle of water near the sample in a shielded stretching chamber throughout the experiment. After every stretching step, 10 min was allowed for structural equilibration. The SANS measuring time was 10 min for the case of SDD = 2.00 m and 2 h for SDD = 8.00 m. No significant weight loss due to drying was observed during SANS measurement.

Results and Discussion

1. Mechanical Properties. Figure 1 shows the tensile stress−stretching ratio curves of NC gels and OR gel. The extensibility and the tensile stress of NC gels are much larger than that of OR3 regardless of C_{clay}. Note that, however, the tensile modulus of OR3 is also much larger than those of NC gels. These facts can be explained as follows. Because the numbers of clay platelets in NC2, NC4, and NC6 are much smaller than those of cross-linker (BIS) in OR3, the molecular weight of polymer chains between cross-linkers in NC gels is obviously larger than

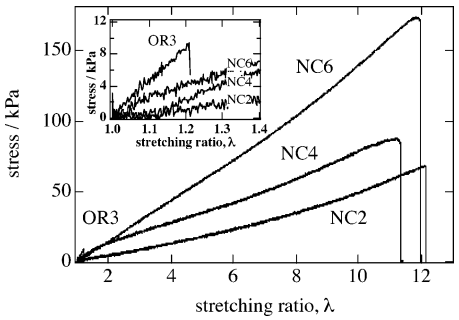

Figure 1. Stress−stretching ratio curves of NC2, NC4, and NC6 (nanocomposite gel cross-linked with clay) and OR3 (conventional chemical gel cross-linked with BIS).

that of OR3 and the cross-link inhomogeneities are smaller. Besides, with increase the C_{clay}, the tensile stress and the tensile modulus increase as shown in Figure 1. This systematic change is also interpretable as mentioned above. That is, an increase of C_{clay} makes the inter clay distance smaller and then cross-link density larger.

Note that an interesting recovery behavior was observed after stretching, i.e., first quick but not complete recovery and subsequent very slow recovery as reported in our previous paper.[10] As a matter of fact, an NC gel recovers its initial length through a process having two different time scales. Haraguchi et al. reported this interesting recovery behavior of NC gels as a function of C_{clay} up to $C_{clay} = 0.20$ M (NC20). [8] They reported that NC gels with high C_{clay}'s, such as NC10 and more, cannot recover their initial size after large deformation. This is due to different orientation behaviors of clay platelets depending on the stretching ratio below or above $C_{clay} = 0.10$ M (NC10). In our case, the values of C_{clay} are 0.02 (NC2), 0,04 (NC4), and 0.06 (NC6) and are lower than the threshold. Hence, it is reasonable that these gels recovered their initial size after deformation.

2. SANS Experiment. Two-Dimensional Pattern. Since NC gels are three-component systems, consisting of clay, PNIPA, and solvent, the scattering intensity function is obtained as follows:[15]

$$I(q) = \phi_P\phi_S(\rho_P - \rho_S)^2 S_{PP} + \phi_C\phi_S(\rho_C - \rho_S)^2 S_{CC} + 2\phi_P\phi_C(\rho_P - \rho_S)(\rho_C - \rho_S)S_{PC} \quad (1)$$

where ϕ_i and ρ_i indicate the volume fraction and the scattering length density of each component, i (P, PNIPA; C, clay; S, solvent), respectively. $S_{PP}(q)$, $S_{CC}(q)$, and $S_{PC}(q)$ are the polymer−polymer, clay−clay, and polymer−clay structure factors, respectively. If one uses a solvent whose scattering length density is equal to that of clay ($\rho_S = \rho_C$; contrast matched), eq 1 becomes

$$I(q) = \phi_P\phi_S(\rho_P - \rho_S)^2 S_{PP} \quad (2)$$

Hence, the polymer−polymer structure factor can be exclusively obtained by using a contrast-matched solvent. Figure 2 shows the two-dimensional scattering patterns of uniaxially stretched NC2, taken with SDD = 8 m. The upper columns are the case of D_2O solvent and the lower columns are the case of the contrast-matched solvent. The stretching direction was horizontal. As shown in the figures, the scattering pattern changes with stretching. At the beginning ($\lambda = 1.0$), the scattering pattern is isotropic. By increasing λ, the scattering pattern represents two distinct features. The first is that the peripheral region of the pattern at $\lambda = 6.0$ is an elliptic shape with their long axis

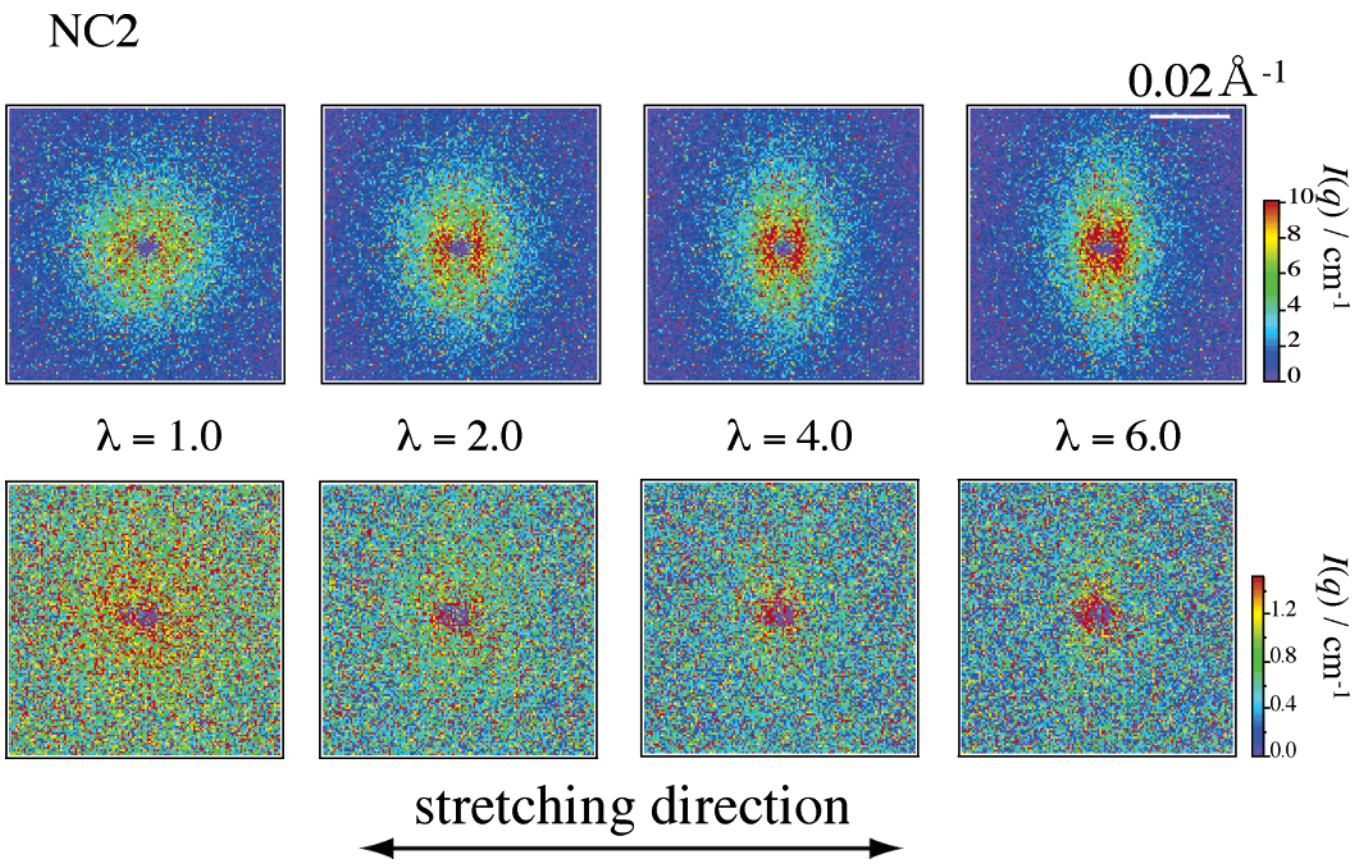

Figure 2. Two-dimensional SANS patterns for NC2 (SDD = 8 m): (top) in D_2O solvent; (bottom) in contrast matched solvent. λ is the stretching ratio.

oriented perpendicular to the stretching direction (blue). The second is that the central part is a two-lobe pattern strongly oriented parallel to the stretching direction (red). The central pattern is similar to the so-called "abnormal-butterfly" pattern, which is often observed from stretched chemical gel with large cross-link inhomogeneities.[16,17] Though a "abnormal-butterfly-like" pattern was observed both in D_2O and in the contrast matched cases, such patterns were more clearly observed in NC4 and NC6.

Figure 3 shows the two-dimensional scattering patterns of uniaxially stretched NC4. The SANS patterns clearly show the characteristic features and the effects of contrast matching are more distinct than those of NC2. Even in the case of contrast-matched sample, the scattering patterns accompanying two lobes in the stretching direction are clearly observed. Since clay platelets are supposed to be "invisible", this two-lobe pattern must be ascribed to an anisotropic scattering from deformed polymer chains. However, this two-lobe pattern is partially ascribed to the "invisible" platelets as will be discussed later. At the high-q region, on the other hand, the SANS pattern stretched in the perpendicular direction is interpreted to be due to elongated polymer chains along the parallel direction. This is due to deformed polymer chains by stretching. Hence, by combining ordinary and contrast-matched SANS, one can differentiate the two contributions, i.e., clay platelet orientation and polymer chain stretching.

In Figure 4 (NC6), the effects of stretching are more amplified both in the case of D_2O (upper column) and the contrast matched solvent (lower). In the case of the former, both clay and PNIPA chains are visible by SANS. Hence, it is reasonable that the effects of stretching are much amplified than the case of NC2 and NC4. On the other hand, since only PNIPA chains are visible in the contrast-matched solvent, effects of clay concentration is not expected to appear in the SANS pattern in the lower column. However, it is clear that the SANS patterns for NC gels in the contrast matched solvent is C_{clay}-dependent as well as λ dependent. Therefore, it is worthy to discuss this issue. In the latter section, we investigate the scattering patterns obtained from a contrast-matched solvent to extract information on deformed PNIPA chains.

Undeformed State. It is well-known that the scattering function from a semidilute−polymer solution, $I(q)$, is given by the so-called Ornstein−Zernike (OZ) function[18]

$$I(q) = \frac{I(0)}{1 + \xi^2 q^2} \tag{3}$$

Here, ξ is the characteristic correlation length and $I(0)$ is the initial scattering intensity. The scattering intensity from conventional chemical gels which have large cross-link inhomogeneities is represented by a sum of Lorentz function and squared-Lorentz function.[19,20] Figure 5 shows OZ plots for circular-averaged scattering intensities obtained from the two-dimensional SANS patterns of $\lambda = 1.0$ for the case of the contrast matched solvent. In these plots, each data set was well represented by a straight line, representing the concentration fluctuations are essentially the same as those of polymer solutions. In other words, these plots indicate that the NC gels have very small cross-link inhomogeneities regardless of C_{clay}. Hence the PNIPA chains in NC gels behave in a manner similar to that of polymer solutions.

Figure 6 shows C_{clay} dependence of (a) the correlation length ξ and (b) the initial scattering intensity $I(0)$. The correlation length ξ decreased with increasing C_{clay}. Though $I(0)$ is known to be proportional to $\phi_P\xi^3$ for semidilute polymer solutions,[18] ϕ_P is almost constant in this work. Here, ϕ_P is the volume

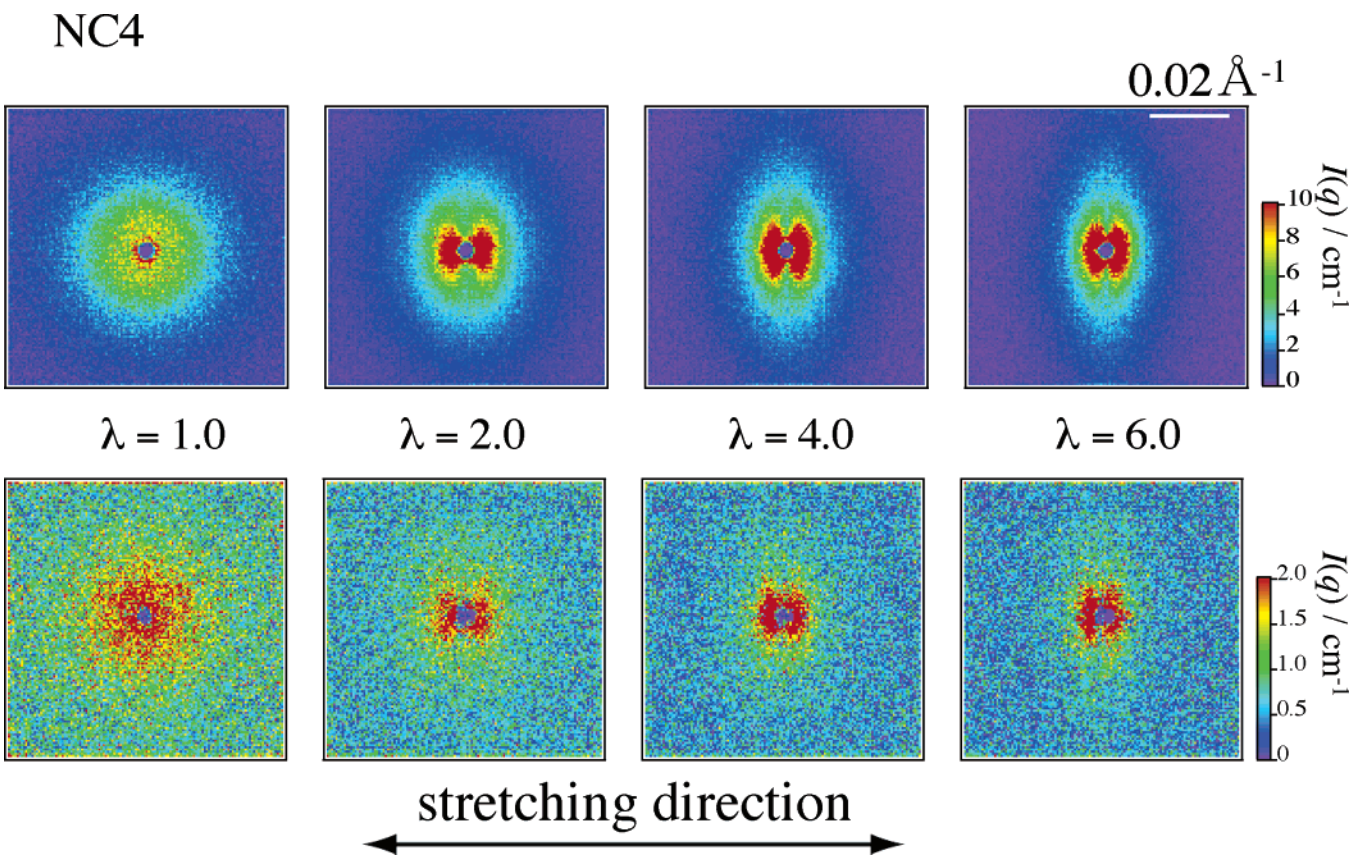

Figure 3. Two-dimensional SANS patterns for NC4 (SDD = 8 m): (top) in D_2O solvent; (bottom) in contrast matched solvent.

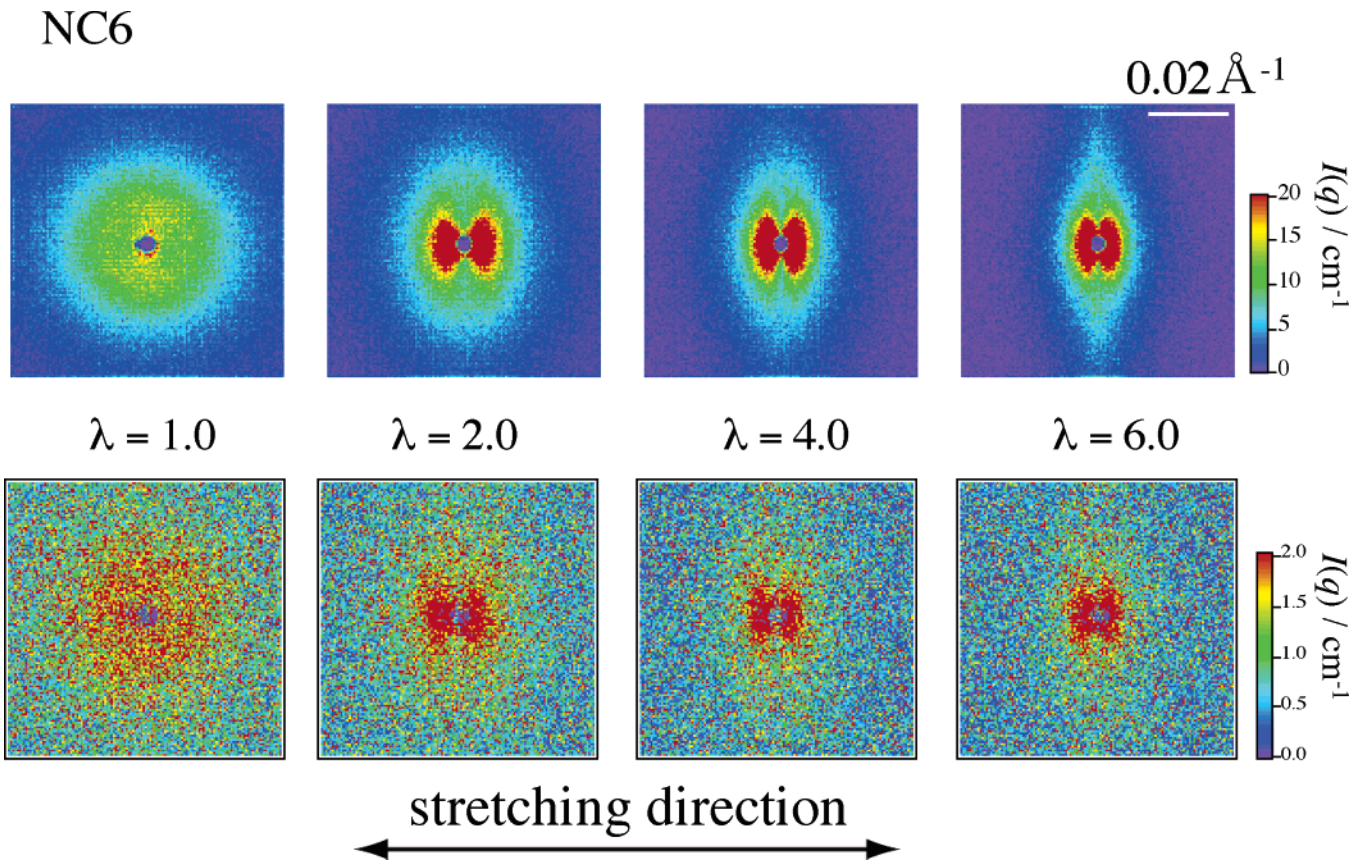

Figure 4. Two-dimensional SANS patterns for NC6 (SDD = 8 m): (top) in D_2O solvent; (bottom) in contrast matched solvent.

fraction of the polymer. Hence, neither ξ nor $I(0)$ is expected to vary with C_{clay} if the system is a mere semidilute polymer solution and clay platelets play just as additives. This conjecture is obviously contradictory to the experimental result. This means that the presence of clay platelets plays significant role in the microscopic structure of NC gels. With increasing C_{clay}, the

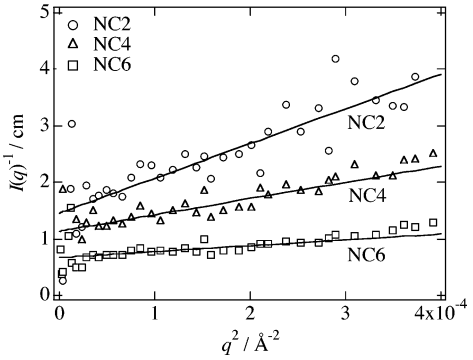

Figure 5. OZ plots of circular-averaged SANS intensity function for NC2, NC4, and NC6 ($\lambda = 1.0$). The solid lines are the fitting results with OZ function.

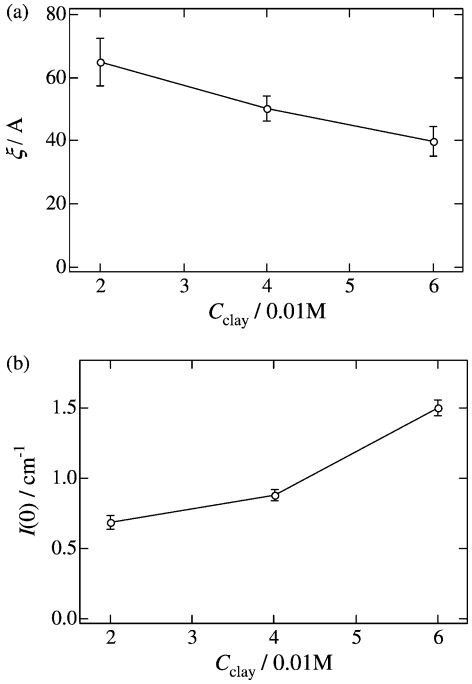

Figure 6. C_{clay} dependence of (a) the correlation length and (b) the zero-q intensities.

interclay distance decreases and then the blob size of PNIPA chain is expected to decrease. As a result, ξ decreases and $I(0)$ should decrease accordingly. However, the observed initial scattering intensity $I(0)$ increased with increasing C_{clay}. To account for the increase in $I(0)$ with C_{clay}, it is necessary to propose a model in which clay scattering does exist. Clay platelets themselves are invisible because of contrast matching. However, they can be visualized by decoration. Haraguchi et al. reported that in the process of mixing of clay and NIPA monomer, considerable amount of monomers are adsorbed on the platelet surface and form "brush particles" in the beginning of polymerization.[6] We believe that this is the reason for the increase of $I(0)$ with increasing C_{clay}. Haraguchi et al. also reported that the polymerization conversion is almost 100% and no sol-fraction from NC gel being extracted.[5]

Let us estimate the average inter-clay-platelet distance, d_{clay}. By assuming equi-distance distribution of clay platelets, one obtains

$$d_{clay} = \left(\frac{V_{clay}\rho_{clay}}{m_{clay}C_{clay}}\right)^{1/3} \tag{4}$$

where V_{clay}, ρ_{clay}, and m_{clay} are the volume, the mass density, and the monomer-equivalent molar mass of clay platelet, respectively. Here we assume that $V_{clay} = 7.07 \times 10^5$ Å^3 (a clay platelet of 300 Å in diameter and 10 Å thick).[3] Figure 7 shows the C_{clay} dependence of d_{clay}, the correlation length ξ_{SANS} from OZ fitting from SANS experiments, and the correlation length ξ_{DLS} obtained by the results of DLS and the Einstein−Stokes equation as follows:[21,22]

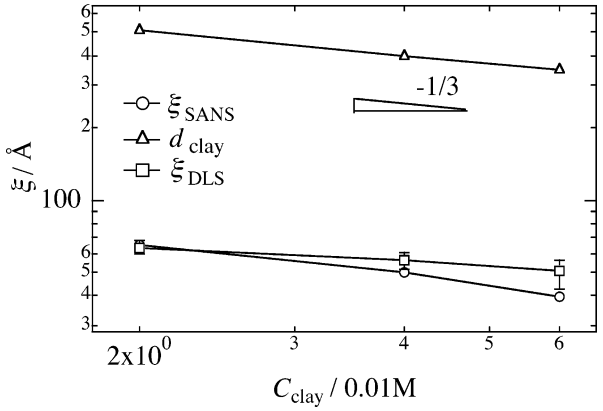

Figure 7. C_{clay} dependence of ξ_{SANS}, d_{clay}, and ξ_{DLS}.

$$\xi_{DLS} = \frac{k_B T}{6\pi\eta D} \tag{5}$$

Here, k_B is Boltzman's constant, T is the absolute temperature, η is the viscosity of solvent, and D is the diffusion coefficient of cooperative diffusion. From the definition, i.e., eq 4, d_{clay} scales with $C_{clay}^{-1/3}$. Interestingly, both ξ_{SANS} and ξ_{DLS} are almost equal and decrease with a similar fashion as that of d_{clay}, i.e., $\xi_{SANS} \approx \xi_{DLS} \sim C_{clay}^{-1/3}$. This means that the correlation of concentration fluctuations in NC gels is effectively screened by clay platelets.

Haraguchi et al.[4] evaluated three characteristic number densities related to the structure of NC gels, i.e., the number of clay platelets in a unit volume, N_{clay}, the number of effective PNIPA chains per unit volume responsible for sustaining external mechanical force, N_{chain}, and the number of PNIPA chains anchored to a clay platelet, N^*. N_{clay} was simply obtained by C_{clay} and the volume of clay platelet. On the other hand, N_{chain} was evaluated from their mechanical measurements by using the kinetic theory of rubber elasticity:[23]

$$F = \Phi N_{chain} k_B T\{\lambda - \lambda^{-2}\} \tag{6}$$

Here, F is the force per unit original (undeformed) cross-sectional area of the network. Φ, which is called the front factor, is related to the specifics of the cross-linking process and chains. In this case, Φ is considered to be close to unity. N^* was obtained by taking the ratio, N_{chain}/N_{clay}. Figure 8a shows the C_{clay} dependence of N_{chain} and N_{clay}. It is trivial that N_{clay} is proportional to C_{clay}, i.e., $N_{clay} \sim C_{clay}$. However, it is noted that N_{chain} was found to scale with $C_{clay}^{4/3}$. In the case of elastomers and conventional gels, the number of effective chains sustaining external force is proportional to the cross-linker concentration, C_x.[24] Hence, the relationship $N_{chain} \sim C_{clay}$ is conjectured instead of $N_{chain} \sim C_{clay}^{4/3}$. The additional $C_{clay}^{1/3}$ dependence of N_{chain} is ascribed to the "plane cross-linking"[10] rather than a "point cross-linking" in conventional gels. Let us discuss this issue in the following.

In Figure 8b, the number of PNIPA chains anchored to one platelet, N^*, is plotted as a function of C_{clay}. N^* is an increasing

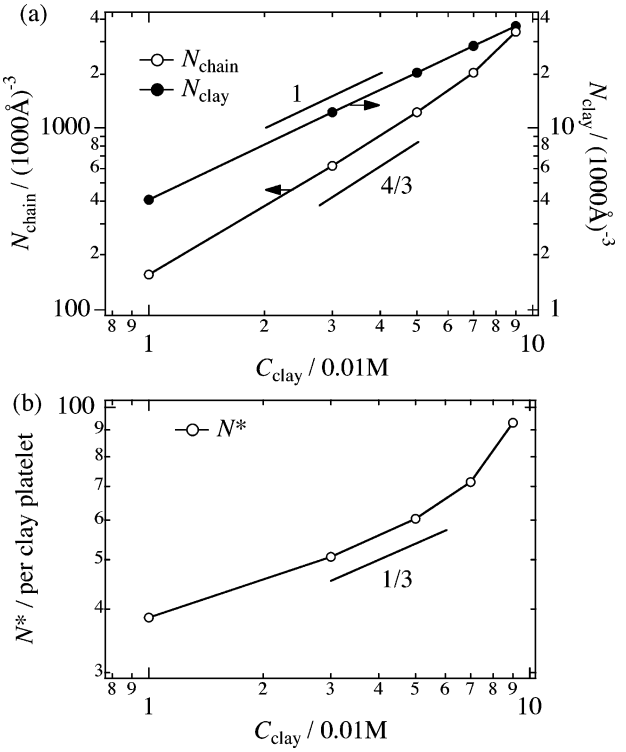

Figure 8. C_{clay} dependence of (a) N_{chain}, N_{clay}, and (b) N^*.

function of C_{clay}, and the values of N^* are of order of 50 to 100. The scaling argument given in the previous paragraph leads to the following,

$$N^* \equiv \frac{N_{chain}}{N_{clay}} \sim \frac{C_{clay}^{4/3}}{C_{clay}} \sim C_{clay}^{1/3} \qquad (7)$$

This means that surface densification on platelets occurs by increasing C_{clay}. Note that the correlation length is a decreasing function of C_{clay} with a fashion of $\xi_{SANS} \sim C_{clay}^{-1/3}$(Figure 7), which indicates a three-dimensional scaling, i.e., $\xi^3 C_{clay}$ being constant. This suggests that a gel consists of volume-filled blobs. This type of relationship also applies to the number of cross-links and blobs in the case of conventional gels. However, this statement cannot be applied to NC gels because the product $C_{clay}\xi/N^*$ is not proportional to C_{clay}^0 but to $C_{clay}^{1/3}$. This is due to the fact that cross-links are not dispersed in a three-dimensional space in gels but are localized on a two-dimensional space, i.e., on the surface of clay platelets. This allows the NC gels to have long PNIPA chains whose ends are anchored on clay platelets. As a result, NC gels achieve exceptionally high extensibility.

On the basis of the above discussion, we schematically drew microscopic structures of NC gels in Figure 9. In this figure, only small numbers of PNIPA chains are drawn for the purpose of simplicity. The volume of the compartment partitioned to one clay platelet is calculated from the size of the platelet and the density of the clay. The size of the compartment is larger than the platelet diameter while $C_{clay} < 0.10$ M (NC10), but becomes smaller than the platelet diameter for $C_{clay} > 0.10$ M. Besides, with increasing C_{clay}, the number of PNIPA chain bridging platelets increases (See N^* in Figure 8b). The circles indicate blobs with the size ξ, which decreases with increasing C_{clay} (Figure 7).

Stretched State. When NC gels are stretched ($\lambda > 1.0$), the scattering patterns become anisotropic. A sector average was taken with the angle of ±10° along the horizontal (parallel) and

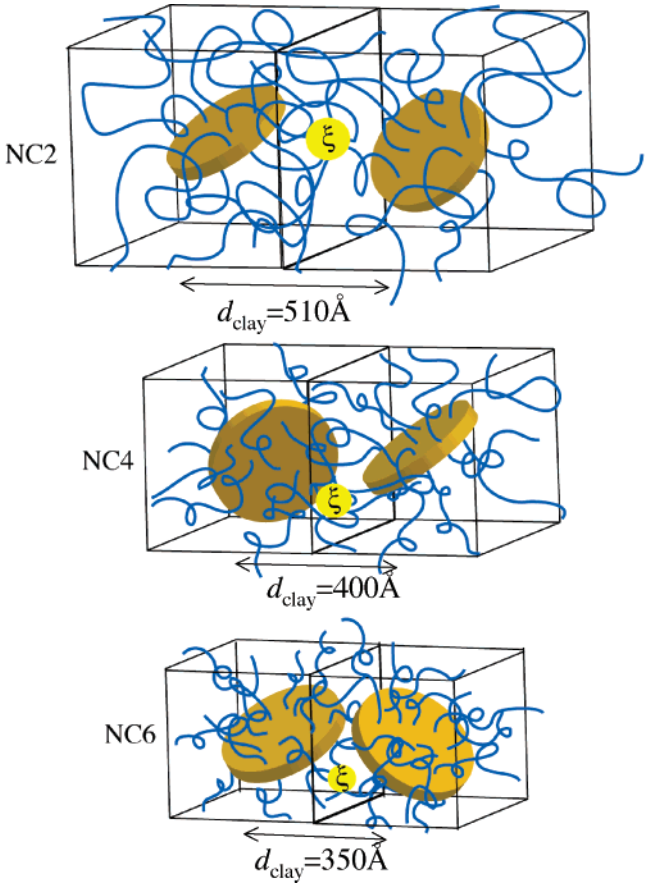

Figure 9. Schematic representation of NC2, NC4, and NC6. The brown disks, blue lines, cubes, and yellow circles indicate clay platelets, PNIPA chains, compartments that one clay platelet can occupy, and blobs, respectively.

vertical (perpendicular) directions. Both sector-averaged scattering intensities, $I_{para}(q)$ (parallel) and $I_{perp}(q)$ (perpendicular), were well represented by OZ functions. This indicates that inhomogeneities in NC gels are insignificant even in stretched state. This result is in accordance with the fact that stretching does not decrease the transparency (visual observation). In the case of conventional chemical gels, on the other hand, cross-link inhomogeneities increase preferentially in the stretching direction. The two-lobe pattern in the two-dimensional scattering patterns is originated from the scattering contrast created by adsorbed PNIPA chains on clay platelets. The two-lobe patterns appear preferentially in the stretching direction, indicating that the clay platelets are oriented with their surface normals parallel to the stretching direction.

Figure 10 shows the fitting results, ξ_{para} and ξ_{perp} vs λ, for NC2, NC4, and NC6 in the contrast-matched solvent. ξ_{para} and ξ_{perp} are the correlation lengths from $I_{para}(q)$ and $I_{perp}(q)$, respectively. Regardless of C_{clay}, ξ_{para} increases with increasing λ. On the other hand, ξ_{perp} slightly changes with increasing λ. This can be explained as follows. The clay platelets come to orient with their surface normals parallel to the stretching direction. In NC gels with large C_{clay}'s, clay platelets are so densely packed that the clay platelets do not orientate with their normals along with the stretching direction, but have a tendency to orient with their normals perpendicular to the stretching direction.[8]

Figure 11 shows $I_{para}(0)$ and $I_{perp}(0)$ vs λ, for NC2, NC4, and NC6. $I_{para}(0)$ and $I_{perp}(0)$ are the scattering intensities of $I_{para}(q)$ and $I_{perp}(q)$ at $q = 0$. $I_{para}(0)$ and $I_{perp}(0)$ change similarly to ξ_{para} and ξ_{perp}, respectively. As mentioned in the previous

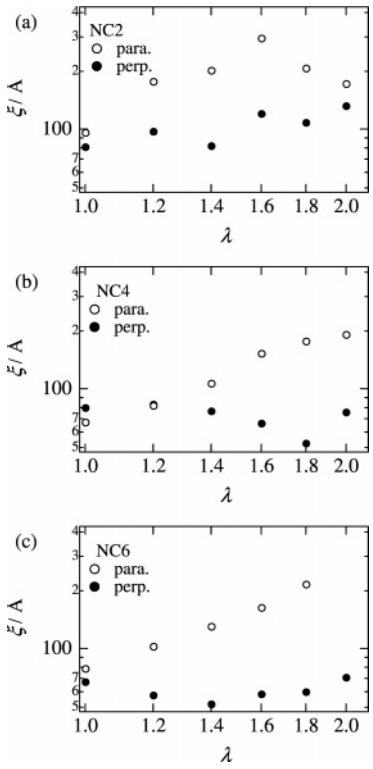

Figure 10. λ dependence of correlation lengths of (a) NC2, (b) NC4, and (c) NC6 parallel and perpendicular to the stretching direction.

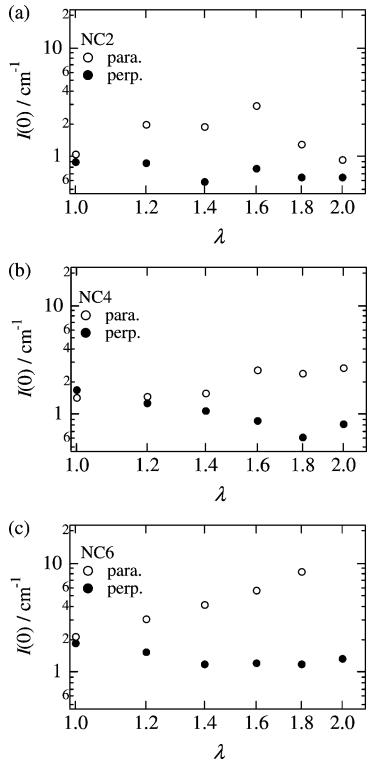

Figure 11. λ dependence of zero-q intensities of (a) NC2, (b) NC4, and (c) NC6 parallel and perpendicular to the stretching direction.

section, $I_{para}(0)$ and $I_{perp}(0)$ are proportional to $\phi_P\xi_{para}^3$ and $\phi_P\xi_{perp}^3$, respectively. It is noted that ϕ_P is the same for parallel and perpendicular directions and almost constant regardless of C_{clay}. Thus, the increase in $I_{para}(0)$ and the decrerase in $I_{perp}(0)$ with increasing λ are due to an increase in ξ_{para} and a decrease in ξ_{perp}, respectively. It is notable that the two-lobe patterns obtained from stretched NC gels are well represented by OZ

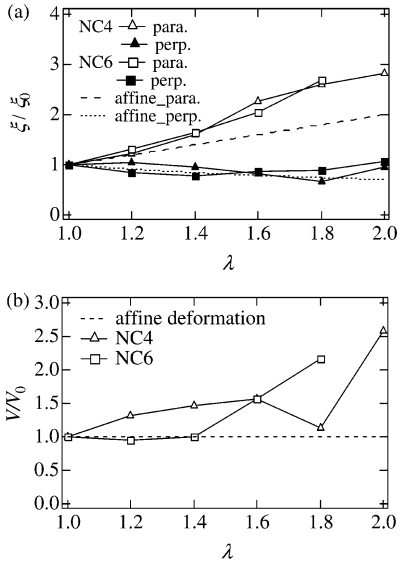

Figure 12. λ dependence of (a) Normalized correlation lengths of NC4 and NC6 parallel and perpendicular to the stretching direction and (b) normalized volume of blobs. The dashed lines indicate the calculation from affine deformation.

function for sector averaged scattering intensity for parallel and perpendicular to the stretching direction and the anisotropy is not originated from cross-link inhomogeneities but from anisotropically deformed blobs. In the previous paper,[10] we proposed the existence of "ghost" scattering. However, the scattering length density of clay in the contrast-matched solvent is not the same as that in PNIPA−D_2O solution but the same as that in the solvent. Then, the difference of the scattering length densities between clay and PNIPA solution in the contrast-matched solvent leads to the "ghost" scattering of clay. Certainly, the ghost scattering can exist, but the contrast is not large enough to be observed by the scattering from the deformed blob. Hence the scattering pattern like "abnormal-butterfly" pattern is originated from the deformed blobs and from an orientation of PNIPA chain near the anchoring point on the clay surface.

Figure 12a shows the λ dependence of the normalized correlation length ξ_{para}/ξ_0 and ξ_{perp}/ξ_0 for NC4 and NC6. Here, ξ_0 is the correlation length with $\lambda = 1.0$ for each sample. The results of NC2 are not shown because of low reliability in the evaluation of ξ's which originates from low statistics in the scattering intensities. Theoretical curves of deformation based on an affine deformation model are also plotted. In this case, ξ_{para}/ξ_0 and ξ_{perp}/ξ_0 are proportional to λ and $\lambda^{-1/2}$, respectively. Both ξ_{para}s and ξ_{perp}s deviate from the results of affine deformation model. Though the reason for this deviation is not clear, the macroscopic deformation is well correlated to the microscopic deformation. In Figure 12b, λ dependence of microscopic volume changes $V/V_0 = (\xi_{para}/\xi_0)\times(\xi_{perp}/\xi_0)^2$ and that of affine deformation are plotted. In the case of affine deformation, V/V_0 remains to be nearly unity irrespective of stretching ratio. This result indicates that clay platelets in an NC gel change their orientation by keeping the microscopic volume of NC gel.

Figure 13 shows schematic illustration of NC gels in stretched state ($\lambda = 2.0$). Here, we demonstrate that each clay platelet is partitioned in a different compartment and orients by rotating its normal parallel to the stretching direction. Clay platelets play as "plane" cross-links, resulting in tying a large number of PNIPA chains. According to Haraguchi et al., this type of orientation becomes impossible when the clay concentration is

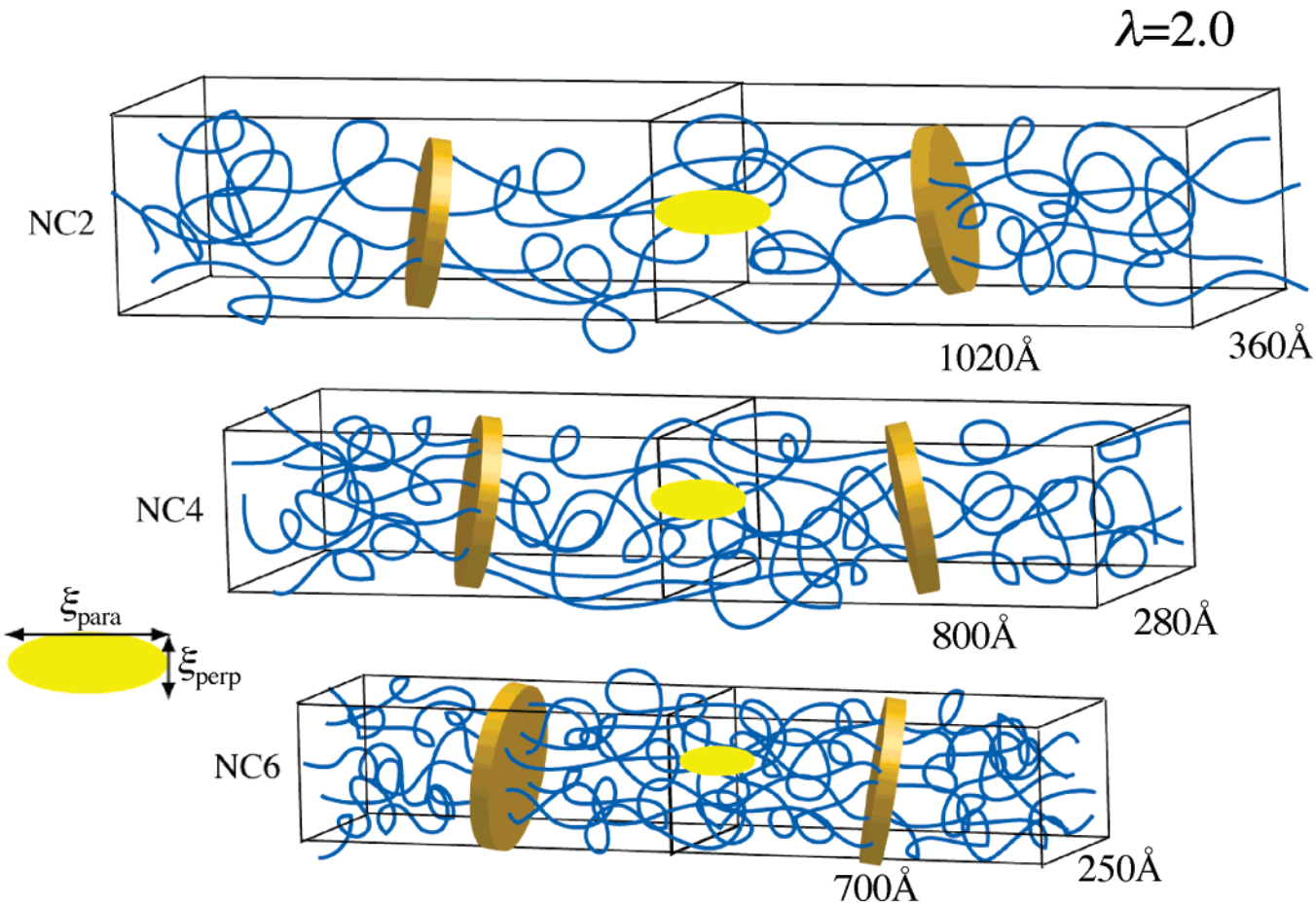

Figure 13. Schematic representation of stretched NC2, NC4, and NC6 ($\lambda = 2.0$).

higher than $C_{clay} > 0.10$ M, and opposite type of orientation takes place.[8] Microscopic verification of such deformation of NC gels will be investigated shortly.

Conclusion

Microscopic structures of NC gels with three different C_{clay}s are investigated by mechanical measurements and SANS in D_2O solvent as well as in a contrast matched solvent with clay. The following facts were disclosed. (1) According to mechanical measurements, both the tensile modulus and tensile strength increase with increasing C_{clay}. Applying the theory of rubber elasticity to the results, it was found that the number of PNIPA chains bridging clay platelets, N^*, increases with increasing C_{clay}. (2) Two-dimensional SANS patterns at $\lambda = 1.0$ show isotropic pattern regardless of C_{clay}. The circular averaged scattering intensity function is well represented by OZ function, which indicates insignificant level of cross-link inhomogeneities in NC gels. (3) The correlation length ξ obtained from OZ fitting decreases with increasing C_{clay} with $\xi \sim C_{clay}^{-1/3}$. (4) The number of effective PNIPA chains per unit volume, N_{chain}, sustaining external forces increases C_{clay} with $N_{chain} \sim C_{clay}^{4/3}$. The additional C_{clay} dependence, i.e., $C_{clay}^{1/3}$ is due to localization of cross-links to the two-dimensional space on clay platelets. This is one of the direct evidence of "plane" cross-linking. (5) Two-dimensional scattering patterns for stretched NC gels show two distinct features from both the D_2O and contrast matched cases. One, an elliptic pattern with their long axis oriented perpendicular to the stretching direction represents the deformation of PNIPA chains, and the other, two-lobe patterns strongly orient parallel to the stretching direction, correspond to deformed blobs and orientation of clay platelets, respectively. (6) Both of the sector-averaged scattering functions for the parallel and perpendicular directions are also well represented by OZ function. It indicates that cross-link inhomogeneities remain significantly low even in the stretched state. (7) The deformed blob sizes ξ_{perp} and ξ_{para} were obtained from fitting of SANS results for stretched state. The volume of blob remains unchanged by stretching.

Acknowledgment. This work is supported by Core Research for Evolutional Science and Technology (CREST), Japan Science and Technology Agency, Japan. T.K. acknowledges the support by CREST. This work was partially supported by the Ministry of Education, Science, Sports and Culture, Japan (Grants-in-Aid 16350120 and 18205025)). The SANS experiment was performed with the approval of Institute for Solid State Physics, The University of Tokyo (Proposal Nos. 5.214, 06.237), at Japan Atomic Energy Agency, Tokai, Japan.

References and Notes

(1) Schmidt, H. In *Polymer Based Molecular Composites*; Schaefer, D. W., Mark, J. E., Eds.; Mater. Res. Soc.: Pittsburgh, PA, 1990; p 3.
(2) Novak, B. M. *Adv. Mater.* **1993**, *5*, 422.
(3) Haraguchi, K.; Takeshita, T. *Adv. Mater.* **2002**, *14*, 1120−1124.
(4) Haraguchi, K.; Takeshita, T.; Fan, S. *Macromolecules* **2002**, *35*, 10162−10171.
(5) Haraguchi, K.; Farnworth, R.; Ohbayashi, A.; Takehisa, T. *Macromolecules* **2003**, *36*, 5732−5741.
(6) Haraguchi, K.; Li, H.-J.; Matsuda, K.; Takehisa, T.; Elliot, E. *Macromolecules* **2005**, *38*, 3482−3490.
(7) Haraguchi, K.; Taniguchi, S.; Takehisa, T. *ChemPhysChem.* **2005**, *6*, 238−241.
(8) Haraguchi, K.; Li, H.-J. *Macromolecules* **2006**, *39*, 1898−1905.

(9) Shibayama, M.; Suda, J.; Karino, T.; Okabe, S.; Takehisa, T.; Haraguchi, K. *Macromolecules* **2004**, *37*, 9606−9612.
(10) Shibayama, M.; Karino, T.; Miyazaki, S.; Takehisa, T.; Haraguchi, K. *Macromolecules* **2005**, *38*, 10772−10781.
(11) Nie, J.; Du, B.; Oppermann, W. *J. Phys. Chem. B* **2006**, *110*, 11167−11175.
(12) Nie, J.; Du, B.; Oppermann, W. *Macromolecules* **2005**, *38*, 5729−5736.
(13) Okabe, S.; Nagao, M.; Karino, T.; Watanabe, S.; Adachi, T.; Shimizu, H.; Shibayama, M. *J. Appl. Crystallogr.* **2005**, *38*, 1035−1037.
(14) Shibayama, M.; Nagao, M.; Okabe, S.; Karino, T. *J. Phys. Soc. Jpn.* **2005**, *74*, 2728−2736.
(15) Higgins, J. S.; Benoit, H. C. *Polymers and Neutron Scattering*; Clarendon Press: Oxford, U.K., 1994.
(16) Boue, F.; Bastide, J.; Buzier, M. In *Molecular Basis of Polymer Networks*; Baumgartner, A., Picot, C. E., Eds.; Springer: Berlin, 1989; p 65.
(17) Ramzi, A.; Zielinski, F.; Bastide, J.; Boue, F. *Macromolecules* **1995**, *28*, 3570−3587.
(18) de Gennes, P. G. *Scaling Concepts in Polymer Physics*; Cornell University: Ithaca, NY, 1979.
(19) Onuki, A. *J. Phys. II* **1992**, *2*, 45−61.
(20) Shibayama, M. *Macromol. Chem. Phys.* **1998**, *199*, 1−30.
(21) Tanaka, T.; Hocker, L. O.; Benedek, G. B. *J. Chem. Phys.* **1973**, *59*, 5151−5159.
(22) Tanaka, T. Light scattering from polymer gels. In *Dynamic Light Scattering*; Pecora, R., Ed.; Plenum Publishing: New York, 1985; pp 347−362.
(23) Treloar, L. R. G. *The Physics of Rubber Elasticity*; Clarendon Press: Oxford, U.K., 1975.
(24) Flory, P. J. *Principles of Polymer Chemistry*; Cornell University: Ithaca, NY, 1953.

MA061688O